

SEISMIC HAZARD MAP USING CONTRIBUTION FACTORS OF SEISMIC SOURCES

N NAKAJIMA¹, H KAMEDA², Y ISHIKAWA³ And T OKUMURA⁴

SUMMARY

Seismic hazard maps have been widely used to represent a regional distribution of seismic hazard of an area of interest. In this study, based on the idea of the "probabilistic scenario earthquake (PSE)" proposed by Ishikawa and Kameda, we developed seismic hazard maps in terms of "contribution factor" of individual seismic source. First, the seismic hazard maps in terms of contribution factor of seismic sources are illustrated for Kinki District of Japan in addition to the conventional hazard maps of seismic intensity parameters. Next we discuss the mesh size for appropriate resolution for seismic hazard maps. From the illustration of proposed hazard maps and a closer look at details, it follows that the seismic hazard map in terms of contribution factor of seismic sources can offer useful information on estimating seismic design load, which is not obtained only from the conventional hazard map.

INTRODUCTION

Seismic hazard maps have been widely used to represent a regional distribution of seismic hazard of an area of interest. For this purpose, seismic intensity parameters such as the peak ground acceleration and the peak ground velocity, have been usually used as hazard indices in the conventional hazard maps. Many seismic hazard maps using seismic intensity parameters have been proposed and developed. Examples include Kawasumi Map [Kawasumi, 1951] in Japan and USGS Map [e.g., Frankel, 1995] in the United States. Though hazard maps representing a regional distribution of seismic intensity are useful in engineering, we cannot obtain information on earthquakes which generate such seismic intensity at site. Therefore, it is also important to develop a seismic hazard map representing information on possible earthquakes corresponding to a certain risk probability. Recently, based on the concept of the "deaggregation of seismic hazard"[e.g., Bazzurro and Cornell, 1999], a seismic hazard map using other hazard indices such as M bar [e.g., McGuire, 1995] have been proposed [e.g., Harmsen et al., 1999].

In this study, we use a method of Probabilistic Scenario Earthquake (PSE), which have been proposed by Ishikawa and Kameda [Ishikawa and Kameda, 1993; Ishikawa et al., 1997] and is one method of "deaggregation of seismic hazard". The objective of this study is to propose a methodology of new seismic hazard maps, which use original hazard indices, and to look close the details of the maps.

¹ Structure Dept, Central Research Institute of Electric Power Industry, Abiko, Japan Email: masato@criepi.denken.or.jp

² Disaster Prevention Research Institute, Kyoto University, Kyoto, Japan Email: kameda@imdr.dpri.kyoto-u.ac.jp

³ Institute of Technology, Shimizu Corporation, Tokyo, Japan Email: yutaka@sit.shimz.co.jp, oku@ori.shimz.co.jp

⁴ Institute of Technology, Shimizu Corporation, Tokyo, Japan Email: yutaka@sit.shimz.co.jp, oku@ori.shimz.co.jp

PROBABILISTIC SCENARIO EARTHQUAKE AND THEIR CONTRIBUTION FACTORS

In the seismic hazard assessment, two typical ways are generally used in regard to the future earthquake occurrences. One is the probabilistic seismic hazard analysis (PSHA) and the other is the use of deterministic scenario earthquakes (SE). While most of seismic hazard assessment in Japan had been performed on the basis of the historical earthquakes data before the Kobe Earthquake, in the future PSHA we should consider the active fault data which may represent the low frequency seismic activities. PSHA is useful because it is capable of determining the ground motion intensity corresponding to a target risk level such as an annual probability of exceedance, and has been used as a major tool for the site ground motion estimation. However, they tend to eliminate the information on the physical characteristics of earthquakes such as their magnitude and epicentral locations. In a sense, this can be regarded as an advantage of PSHA, as it greatly simplifies the issue of design seismic load evaluation. With recent increasing demand for dynamic seismic design of structures, the time history of the earthquake ground motions should be determined in addition to the intensity parameter. It is therefore desirable to clarify the magnitude and epicentral location of the typical earthquakes under the specific risk level.

SE, on the other hand, has been used to estimate regional ground motion distributions for urban earthquake hazard mitigation planning as well as the site earthquake ground motion for design of important structures. In such case, the physical characteristics of SE are unique and deterministic, then the time history of the earthquake ground motion can be readily estimated. SE is generally determined from the geological and seismo-tectonic considerations. However, the relationship between SE and a target risk level is not a clear in most cases.

The concept of probabilistic scenario earthquakes (PSE) proposed by Ishikawa and Kameda [Ishikawa and Kameda, 1993, 1997] makes it possible to establish a logical link between PSHA and SE. It is characterized by using the “hazard-consistent magnitude”, “hazard-consistent distance” and “hazard-consistent azimuth” (by Ishikawa and Kameda [Ishikawa and Kameda, 1993]) determined for individual seismic sources that have been identified according to their “contribution factors”. SE can be objectively determined corresponding to the target probability level by use of the concept of PSE. Furthermore in the proposed PSE methodology, the order of PSE calculated for each site can be also assessed by using original parameter “the contribution factor” of a seismic source. The contribution factor of a seismic source is defined as the conditional probability that an earthquake occurs in that seismic source given that the seismic intensity exceeds a certain value at a site. The contribution factor $C_k(p_0)$ is calculated as following equation:

$$C_k(p_0) = \frac{w_k(p_0)}{\sum_{k=1}^n w_k(p_0)} \quad (1)$$

where $w_k(p_0)$ is the annual occurrence rate of earthquakes which occur in seismic source k and generate a seismic intensity exceeding a certain value at a site for a target risk probability p_0 . Thus, when we aim at a certain seismic intensity level (or the seismic intensity value corresponding to a certain risk level), the seismic sources with greater contribution factor can be chosen as the possible sources of scenario earthquakes. Therefore, by drawing seismic hazard maps in terms of contribution factor, one can easily know what seismic source is dominant for the area and/or what area is strongly affected by the seismic source.

MAPPING OF THE CONTRIBUTION FACTOR

In this study, based on the idea of the “probabilistic scenario earthquake (PSE)”, we developed seismic hazard map using “contribution factor” of individual seismic source. As is mentioned above, we can identify important seismic sources that have large values of the contribution factor $C_k(p_0)$ for the prescribed value of p_0 . Therefore, by mapping contribution factors, one can easily know what seismic source is dominant for the area/or what area is strongly affected by the seismic source and grasp of the regional variation of dominant seismic sources quantitatively. Moreover, by seeing the maps using contribution factors and the maps in terms of expected values of seismic intensity together, one can easily understand that the expected value of seismic intensity at each site is affected by several seismic sources. Also, it will be clearly seen that the way each seismic source contributes to the seismic hazard varies depending on the target risk level and on the type of intensity index. Those issues cannot be obtained from the conventional seismic hazard maps and the proposed method of mapping the contribution factors of seismic sources is marked by the above mentioned ability. Authors have already

illustrated the above mentioned characteristics of proposed maps by using relatively coarse mesh [Nakajima, et al., 1998]. In this study, we illustrate and discuss about the details of the hazard maps based on PSE.

HAZARD MODEL FOR ILLUSTRATION

Analytical Model and Conditions

PSHA method

We used the Poisson typed PSHA method in which all earthquakes are assumed to occur according to the stationary Poisson Process in the time domain.

Modeling of seismic sources

Three types of seismic sources i.e., source-areas, interplate large earthquakes occurring along Suruga-Nankai Trough, and inland active faults are considered in this study. The details of modeling of seismic sources are explained as below. Fig.1 shows a polygon-shaped source-areas characterizing the earthquakes occurring randomly in each area. In each source-area, magnitude-frequency relationship is assumed to follow the Gutenberg-Richter relation, and location of earthquakes is assumed to be distributed uniformly and randomly. The historical earthquake-based data are used to calculate the earthquake occurrence rate in each source-area. The area where the seismic hazard maps are drawn in this study is located within source-area No.9 (maximum magnitude $M_u=7.5$). The Nankai earthquakes and the Tokai earthquakes, which occurred along Suruga-Nankai Trough, are modeled as characteristic magnitude earthquake model separately from the source-area. The 3-dimensional shape of fault, such as area and slant, is modeled for both earthquakes and the occurrence rate is calculated to be 0.0087 from the average time interval of four earthquakes which had occurred since 1605. We assume that each magnitude of the two interplate-earthquake models is independent from each other, and its value is uniformly distributed between 8.0 and 8.4. The “seismogenic active fault” proposed by Matsuda [Matsuda, 1990] are used as active fault data, and we add Uemachi fault to the data. Fig.2 shows the distribution of major seismogenic active faults in the Kinki region and Table.1 gives their parameters. Each seismogenic active fault is modeled as a line segment. In PSHA based on the active fault data, it is assumed that an earthquake with a characteristic magnitude occur randomly in time on each active fault model. The earthquake occurrence rate is evaluated from the long term average slip rate and the displacement per seismic event. In this study, as for the long term average slip rate for each active fault model, we adopt the larger one of values in the data published by the Research Group for Active Faults of Japan [the Research Group for Active Faults of Japan, 1991] and values obtained from the active fault surveys which has been actively performed since the Kobe Earthquake as the long term average slip rate of each active fault model. The earthquake occurrence on the active faults also is assumed to follow the stationary Poisson process because there are very few active faults whose activity history have been exactly known.

Attenuation equation

The response spectrum attenuation equation proposed by Annaka et al, [Annaka, Yamazaki and Katahira, 1997] is used in this study. Particularly we employ the equations at two natural period; $T=0.1$ (sec) and 1.0 (sec). Attenuation uncertainty is assumed to follow the logarithmic normal distribution with logarithmic standard deviation of $\zeta =0.66(T=0.1\text{sec})$, $\zeta =0.60(T=1.0\text{sec})$. The response acceleration A (Gal) is formulated as bellows

$$\log A = c_m M + c_n H - c_d \log(R + 0.334 \exp(0.653 M)) + c_0 \quad (2)$$

in which M represents magnitude, H is the depth of the center of the fault, and R is the shortest distance between site and source. In assessing the value of H for active faults, we employ scaling law on the width of the fault and the M_j (JMA magnitude) proposed by Takemura [Takemura, 1998]. The coefficients of the equation are listed in Table 2.

Target probability level and target area for simulation

In this study, seismic hazard maps corresponding to a probability level of $p_0=0.001$ are discussed. Fig.2 shows the rectangle-shaped target area locating on the interval: east longitude [$135^\circ 36'$, $135^\circ 54'$] \times north latitude

[34° 36', 34° 54'] with broken lines. We assess seismic hazard maps for target area located in Kinki district of Japan, because there exists many active faults densely in the area.

EXAMPLE-A SECTION OF WESTERN JAPAN-

Seismic Hazard Maps in terms of Expected Values of Seismic Intensity

Fig.3 shows the contour maps of expected response acceleration (Gal) for return period of 1000 years. The left (Fig.3a) is a map for natural period $T=0.1\text{sec}$, and the right (Fig.3b) is a map for $T=1.0\text{sec}$, respectively. The mesh size for drawing contour lines is 0.012×0.012 degrees.

For 0.1sec response, the value of the response is the highest in the northwest area and the southwest area. The response acceleration gradually declines toward the east. The difference between the highest and the lowest expected response accelerations is 120Gals. The contour lines vary complexly in the west. For 1.0sec response, the expected value is the lowest in the north and the value increases gradually toward south. The difference between the highest and the lowest expected values is 160 Gals, and is slightly greater than the difference in 0.1sec. The contour lines run parallel with the east and west direction, though the lines vary sharply on $135^\circ 37'E$ where Ikoma fault exits. The difference between two maps is characterized by the direction of contour lines.

Seismic Hazard Maps in terms of Contribution Factors of Seismic Sources

In this subsection, we illustrate hazard maps which represent the regional distribution of contribution factors of individual seismic source. The numerals in the maps denote the contribution factors of seismic sources in percent (%).

For 0.1sec response, Fig.4(a)-(f) shows the contour maps of source area No.9, Nankai-Tokai Earthquake, Biwakoseigan fault zone, Uji fault zone, Ikoma fault zone and Median Tectonic Line (MTL) Izumi-Kongo fault zone. The shape of the contour map of source area No.9 is very similar to the map with expected values of response acceleration (Fig.3a). However, the contribution factor is the highest in the southeast, and the lowest where the expected value is the highest. The contribution factor of Nankai-Tokai Earthquake is small and not dominant, as the value is fewer than 5.0% in most of the area. The contribution factor of Biwakoseigan fault zone is the highest in the northeast of the area as the value is more than 10.0%, and the influence extends to the southwest. The contribution factor of Uji fault zone is the highest on the fault, and the value decreases as the distance of site-to-source is larger. However the influence is small as the value is fewer than 5.0%. Ikoma fault zone is dominant in the west as its contribution factor is more than 30.0% near the fault. The influence of MTL Izumi-Kongo is relatively large in the south as its contribution factor is more than 20.0% though the fault is more than 30 kilometers away. Although the contribution of the source area No.9 extends over the area, the influence of a fault is dominant near the fault when its recurrence time is relatively short such as Uji and Ikoma fault zone. Such faults does not necessarily cause large magnitude earthquakes. The dominant source complexly varies in the area for 0.1sec response.

For 1.0sec response, Fig.5(a)-(f) shows the contour maps of the contribution factor of the same seismic sources for $T=0.1\text{sec}$. The influence of source area No.9 is very small as its contribution factor is about 2%. The contribution factor of Nankai-Tokai Earthquake is the highest in the southeast area and it is dominant in the half of the area as its value is more than 50.0%. The contour lines vary sharply in $135^\circ 37'E$ where the influence of Ikoma fault zone is strong and the influence of Nankai-Tokai Earthquake is pushed the south by Ikoma fault zone. The influence of Biwakoseigan and of Uji fault decline when they are compared with the maps for $T=0.1\text{sec}$. The influence of Ikoma also decreases when it is compared with the map for $T=0.1\text{sec}$. The influence of MTL Izumi-Kongo is large in the south as its contribution factor is more than 15.0%. The seismic sources with large magnitude such as Nankai-Tokai Earthquake and MTL Izumi-Kongo is dominant in the area for 1.0sec response.

MESH SIZE FOR APPROPRIATE RESOLUTION

In this section, we discuss the mesh size for appropriate resolution of proposed seismic hazard maps. In the maps, the regional variation of indices is illustrated by contour lines which expresses the intensity of target

parameter, such as peak ground acceleration. The unknown value on intermediate point is estimated by interpolation using the value of the computational result on its neighbor cell. Therefore, the precision of map depends on a mesh size for computation and the important point to note is that we should consider the mesh size for appropriate resolution in drawing hazard maps. First we illustrate five hazard maps which are calculated from five size mesh. In this study, the mesh size of 0.096×0.096 degrees, 0.048×0.048 degrees, 0.024×0.024 degrees, 0.012×0.012 degrees, and 0.006×0.006 degrees are used.

Mesh size

Fig.6(a)-(e) shows the contour maps of the expected values of response acceleration for natural period 0.1sec and for return period 1000year. Each map is calculated from different mesh size, respectively. In the map based on the mesh size of 0.096×0.096 degrees, the accuracy of the hazard map is lost as the contour line is largely different from the contour line of the maps based on the smaller mesh size. In the maps based on the mesh size of 0.048×0.048 degrees and 0.024×0.024 degrees, the regional variation of the expected values of response acceleration can be roughly represented. However, the local variation cannot be represented as precisely as in the maps with small mesh. In the maps based on the mesh size of 0.012×0.012 degrees and 0.006×0.006 degrees, the contour lines of the hazard indices are virtually identical; they vary smoothly and the local variation can be represented precisely.

Effects of mesh size

In the above example, it is illustrated that the mesh size have closer relation to the precision of the map. And it is estimated that the mesh size of 0.012×0.012 degrees and the mesh size of 0.006×0.006 degrees have appropriate resolution for the area where there exists major active faults densely. Therefore, it follows from this example that the mesh size of 0.012×0.012 degrees is sufficient to assess seismic hazard more precisely for the area. However, the mesh size for appropriate resolution can vary according to the hazard model, such as the density of active faults in the area or seismic intensity parameter used to draw the map. It means that we may not necessarily need small mesh of 0.012×0.012 degrees to represent the distribution of hazard indices if there doesn't exist so much faults as in the area of this study. Therefore, the question which we must consider next is how to evaluate quantitatively the precision of the proposed maps corresponding to the mesh size. Fuller discussion on this question will be presented in the later study.

CONCLUSION

The main results of this study can be summarized as follows:

- (1)A method is proposed for the creation of seismic hazard maps based on the concept of Probabilistic Scenario Earthquake.
- (2)Case studies are presented for the specific part of Japan and its usefulness for engineering is demonstrated. The seismic hazard map using "contribution factor" of seismic sources has the ability to illustrate that the dominant seismic sources vary corresponding to a risk probability and time period of seismic motion, even if the expected values of seismic intensity are same at individual site.
- (3)The mesh size for appropriate resolution in the proposed maps are discussed. The small mesh size is necessary to represent precisely regional distribution of hazard indices for the area in which there exists many seismic sources densely.

REFERENCES

- Annaka, T., Yamazaki, F. and Katahira, F. (1997), *Proceedings of the 24th JSCE Earthquake Engineering Symposium*, pp161-164 (in Japanese).
- Bazzurro, P. and Cornell, C.A. (1999), "Disaggregation of Seismic Hazard", *Bulletin of the Seismological Society of America*, 89, 2, pp501-520.
- Frankel, A. (1995), "Mapping Seismic Hazard in the Central and Eastern United States", *Seismological Research Letters*, 66, pp8-21.
- Harmsen, S., Perkins D. and Frankel, A. (1999), "Deaggregation of Probabilistic Ground Motions in the Central and Eastern United States", *Bulletin of the Seismological Society of America*, 89, 1, pp1-13.
- Ishikawa, Y. and Kameda, H. (1993), "Scenario earthquakes vs. probabilistic seismic hazard", *Proc. of Fourth International Conference on Structural Safety and Reliability*, 3, pp2139-2146, Innsbruck, Austria.

Ishikawa, Y., Okumura, T. and Kameda, H. (1997), "Seismic hazard from low frequency-high impact fault activities using probabilistic scenario earthquakes", *Proc. of Fifth International Conference on Structural Safety and Reliability*, 3, pp1519-1524, Kyoto, Japan.

Kawasumi, H. (1951), "Measures of Earthquakes Danger and Expectancy of Maximum Intensity Throughout Japan as Inferred from the Seismic Activity", *Bulletin of the Earthquake Research Institute*, Vol.29, pp469-482

Matsuda, T. (1990), "Seismic zoning map of Japanese islands, with maximum magnitudes derived form active faults data", *Bulletin of Earthquake Research Institute*, University of Tokyo 65, pp289-319 (in Japanese).

McGuire, R.K. (1995), "Probabilistic seismic hazard analysis and design earthquakes: closing the loop", *Bulletin of the Seismological Society of America*, 85, 2, pp1275-1284.

Nakajima, M., Kameda, H, Ishikawa, Y. and Okumura, T. (1998), "Seismic Hazard Map Determined by Probabilistic Scenario Earthquakes Considering Active Faults", *Proc. of the 10th Earthquake Engineering Symposium*, 1, pp151-155 (in Japanese).

Takemura, M. (1998), "Scaling law for Japanese Intraplate Earthquakes in Special Relations to the Surface Faults and the Damages", *Journal of the Seismological Society of Japan*, Vol.51, pp211-228 (in Japanese).

The research group for active faults of Japan (1991), *Maps of active faults in Japan with an explanatory text*, University of Tokyo press (in Japanese).

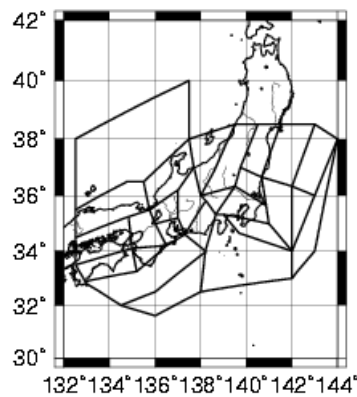


Figure 1: Source area model

Table 1: Parameters of seismogenic active faults in the area

<i>Name of Fault System</i>	Class	T_R (years)	L (km)	M_J	No.
Biwako Seigan	B	1800	34	7.4	1
Uji	B	8000	25	7.2	2
Wazukatani	B	11000	14	6.8	3
Narabonchi nishi	B	6200	20	7.0	4
Ikoma	B	1400	27	7.2	5
Arima-Takatsuki	B	2500	52	7.7	6
Narabonchi Toen	B	5500	21	7.0	7
Yamatogawa	B	6000	19	7.0	8
MTL Izumi-Kongo	A	1000	63	7.8	9

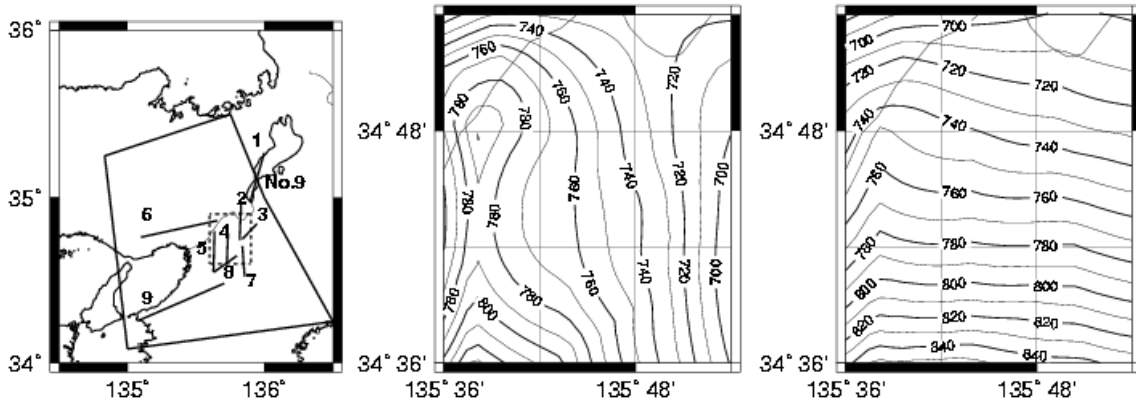
Class : Class of Fault Activity, T_R : Average Recurrence Time

L : Fault Length, M_J : JMA Magnitude, MTL : Median Tectonic

Line

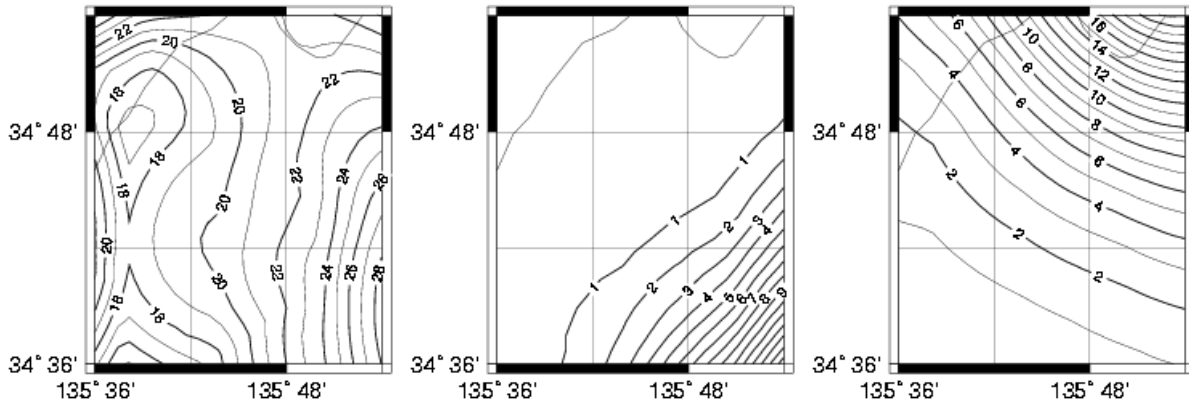
Table 2: Coefficients of attenuation equations

	C_m	C_h	C_d	C_0
$T=0.1\text{sec}$	0.594	0.00543	2.270	2.223
$T=1.0\text{sec}$	0.792	0.00190	1.770	-0.175

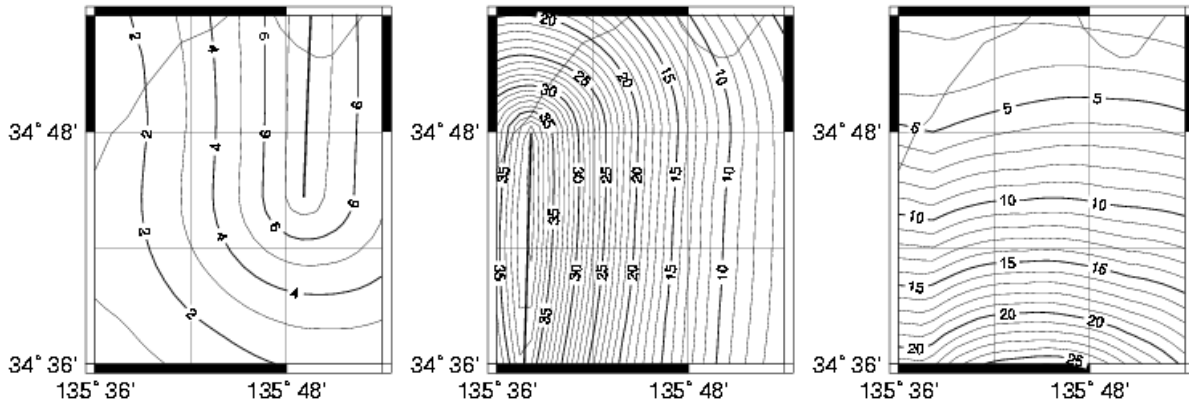


(a)period:0.1sec (b)period:1.0sec

Figure 2: Source area No.9 and major Figure3: Hazard map in terms of expected value of response active faults in Kinki District. Dotted acceleration (unit:Gal, return period:1000year) lines indicate the area to draw the hazard maps.

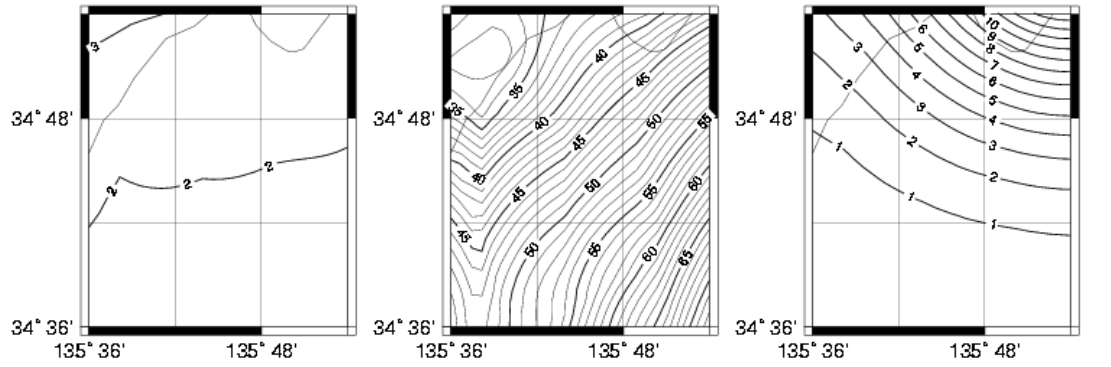


(a)Source area No.9 (b)Nankai-Tokai Earthquake (c)Biwakoseigan fault zone

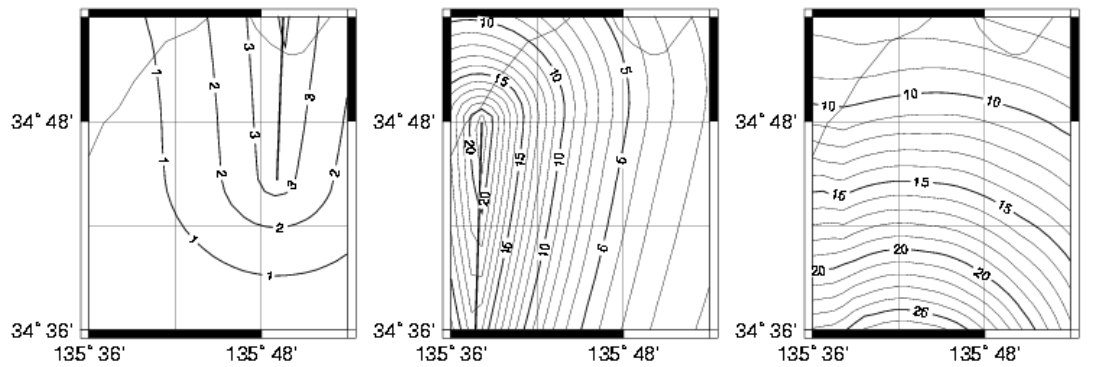


(d)Uji fault zone (e)Ikoma fault zone (f)MTL Izumi-Kongo fault zone

Figure 4: Hazard map using contribution factors of seismic sources (unit: percent, period: 0.1sec, return period: 1000year)

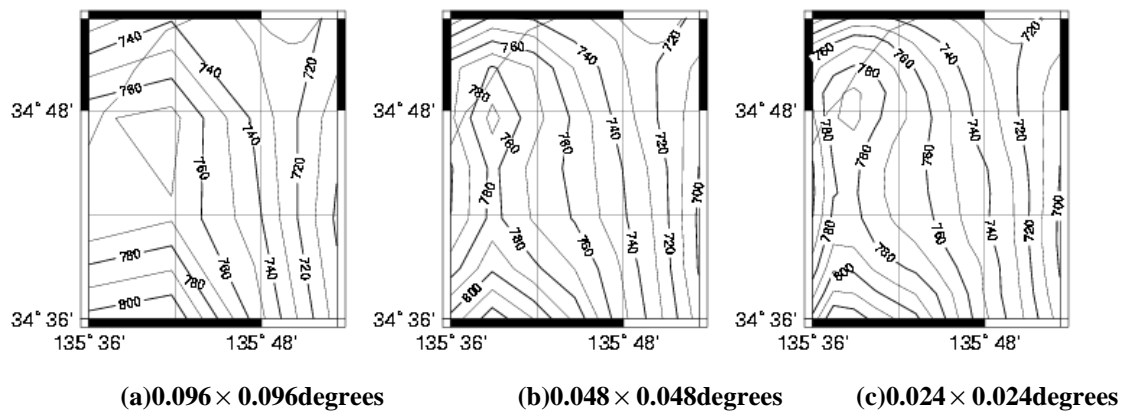


(a)Source area No.9 (b)Nankai-Tokai Earthquake (c)Biwakoseigan fault zone

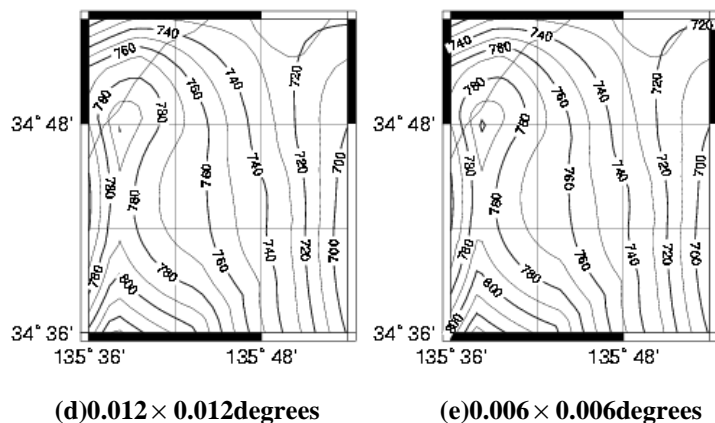


(d)Uji fault zone (e)Ikoma fault zone (f)MTL Izumi-Kongo fault zone

Figure 5: Hazard map using contribution factors of seismic sources
(unit: percent, period: 1.0sec, return period: 1000year)



(a)0.096 x 0.096degrees (b)0.048 x 0.048degrees (c)0.024 x 0.024degrees



(d)0.012 x 0.012degrees (e)0.006 x 0.006degrees

Figure 6: The variation of seismic hazard maps with expected values of response acceleration in varying mesh size (unit: Gal, period: 0.1sec, return period: 1000year)